

Topological defects in antiferromagnetically coupled multilayers with perpendicular anisotropy

N. S. Kiselev^{1,2,*}, U. K. Röbler^{1,†}, A. N. Bogdanov¹, and O. Hellwig³

¹IFW Dresden, Postfach 270116, D-01171 Dresden, Germany

²Donetsk Institute for Physics and Technology, 83114 Donetsk, Ukraine and

³San Jose Research Center, Hitachi Global Storage Technologies, San Jose, CA 95135, USA

A rich variety of specific multidomain textures recently observed in antiferromagnetically coupled multilayers with perpendicular anisotropy include regular (equilibrium) multidomain states as well as different types of *topological* magnetic defects. Within a phenomenological theory we have classified and analyzed the possible magnetic defects in the antiferromagnetic ground state and determine their structures. We have derived the optimal sizes of the defects as functions of the antiferromagnetic exchange, the applied magnetic field, and geometrical parameters of the multilayer. The calculated magnetic phase diagrams show the existence regions for all types of magnetic defects. Experimental investigations of the remanent states (observed after different magnetic pre-history) in [Co/Pt]/Ru multilayers with wedged Co layers reveal a corresponding succession of different magnetic defect domain types.

PACS numbers: 75.70.Cn, 75.50.Ee, 75.30.Kz, 85.70.Li,

Antiferromagnetically coupled [Co/Pt]/Ru, Co/Ir, Fe/Au, [Co/Pt]/NiO multilayers with strong perpendicular magnetic anisotropy represent a new class of synthetic magnetic materials characterized by a cascade of field-driven reorientation transitions, extended regions of metastable states and specific multidomain structures [1, 2, 3, 4, 5, 6, 7]. These spatially inhomogeneous magnetic textures can be separated into two fundamentally different groups. *Regular* multidomain configurations, which correspond to the global or local minima of the systems, and *irregular* networks of domain walls and bands within the antiferromagnetic ground state. The latter are topologically stable inclusions of “old” phases trapped within the equilibrium states. These defects display a large variability and their hysteretic formation strongly depends on the magnetic and temperature pre-history [1, 3, 4, 6, 7].

In this Letter we investigate the field-driven evolution of the regular phases and their topological defects using a basic micromagnetic model for antiferromagnetically coupled multilayers with out-of-plane anisotropy. The calculated magnetic phase diagrams show the stability limits of the regular equilibrium states and indicate the regions where different types of magnetic defects can exist. Magnetization processes can be analysed using these phase diagrams. The approach provides a consistent picture for the formation of specific remanent states in antiferromagnetically coupled multilayers and explains the physical mechanisms for the configurational hysteresis of multidomain states as recently observed in experiments on [Co/Pt]/Ru [2, 4, 6, 7] and [Co/Pt]/NiO [3] multilayers.

Antiferromagnetically coupled Co superlattices investigated in [1, 3, 4, 6, 7] include N “ferromagnetic” blocks composed of X bilayers [Co(h)/M (t)] antiferromagnetically coupled via A (s) spacers (M = Pt, Pd, A = Ru,

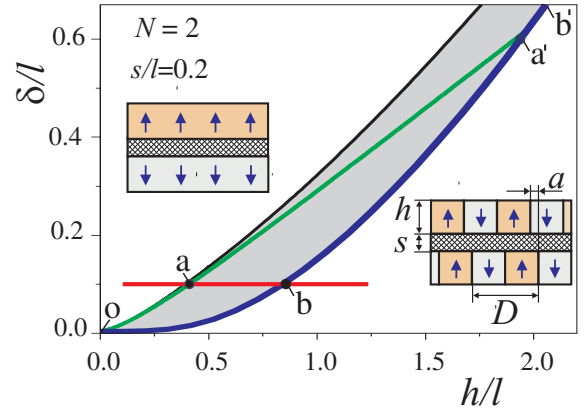


FIG. 1: (Color online) The transition region between the homogeneous antiferromagnetic phase and the ferrostripes. The first-order transition line between these states is shown by a thick (blue) line $o - b - b'$. The ferrostripes are metastable within the shaded area. The ferromagnetic bands (Fig. 3 a) exist between $o - a - a'$ and $o - b - b'$ lines. Thick (red) line $\delta/l = 0.1$ corresponds to the horizontal axis in Fig. 2, $h_a = 0.401$, $h_b = 0.923$.

NiO, Ir) with thicknesses h , t , s of the corresponding nanolayers. Following [5, 8] we write the reduced energy density ($w = W/(2\pi M^2 X N)$) of ferromagnetic stripes as

$$w = \frac{4l}{D} + \frac{\delta}{hX} \left(1 - \frac{1}{N}\right) - \frac{Hq}{2\pi M} + w_m(D, q). \quad (1)$$

The first term in (1) is the domain wall energy, $l = \sigma/(4\pi M^2)$ is the *characteristic* length with domain wall energy density σ , the *exchange length* $\delta = J/(2\pi M^2)$ equals the ratio of the antiferromagnetic coupling $J > 0$ and the stray-field energy, the reduced magnetization $q = (d_1 - d_2)/D$ is defined as ratio of the difference between the widths of up and down domains (d_1 , d_2) and

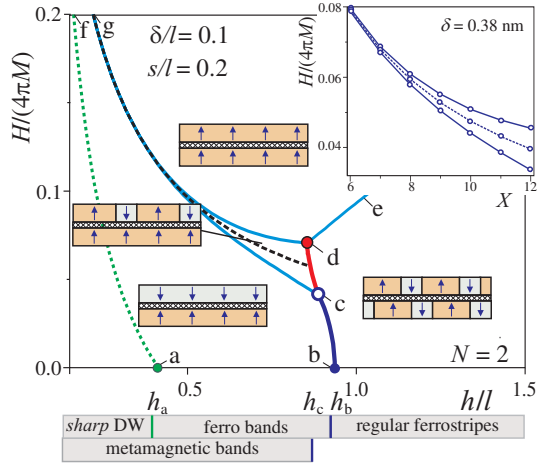


FIG. 2: (Color online) The magnetic phase diagram of the equilibrium states in reduced variables for layer thickness h/l and bias field $H/(4\pi M)$. Metamagnetic stripes exist within area $c-g-d$. The thick line $c-d$ indicates the first-order transition between metamagnetic and shifted ferro stripes. The shifted ferro stripes phase transforms discontinuously into the antiferromagnetic and ferromagnetic phases along lines $b-c$ and $d-e$, correspondingly. The first-order lines meet in the triple points c (0.874, 0.043) and d (0.845, 0.072). The dotted (green) line $a-f$ is the stability limit of the ferromagnetic band defects. The lower panel indicates thickness intervals for the different types of remanent states. The inset shows the region of the magnetic phase diagram for [Co/Pd]/Ru multilayers investigated in Ref. [4].

the domain period $D = d_1 + d_2$. The stray field energy w_m includes the "self" energies of individual layers and the energies of dipolar interactions between them. This can be expressed as a set of finite integrals [8, 10]. The equilibrium domain configurations of the stripes are derived by minimization of w with respect to D and q [8]. The seven control parameters of the model (δ/l , $H/(4\pi M)$, h/l , s/l , t/l , X , N) create a complex multi-dimensional phase diagram of possible solutions. To demonstrate main features of these solutions we consider a simple model for $N = 2$ (Fig. 1). The phase diagram for weak enough interlayer exchange in Fig. 1 contains the antiferromagnetic monodomain or ferrostripe phases. These phases are the possible ground states of the multilayers investigated in [1, 3, 4, 6, 7]. The antiferromagnetic exchange coupling causes a relative shift of domains ($a \propto \delta$) in adjacent layers (Fig. 1). This lateral shift induces the instability of the ferrostripe phase at lower thickness [5] (Fig. 1). In a magnetic field the antiferromagnetic phase transforms into the saturated state via a specific multidomain phase. This is similar to a metamagnetic phase transition in bulk antiferromagnets [11]. In an intermediate (*metamagnetic*) phase domains arise only in one of the ferromagnetic blocks while the other remains in the homogeneous (saturated) state (Fig. 2). In the limit of large domains ($D \gg L$,

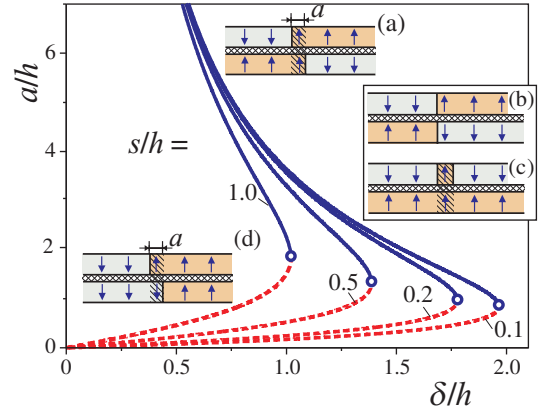


FIG. 3: (Color online) The optimal values of the reduced width a/h for *ferrobands* (a) and *metastable shifted ferrostripes* (d) (dashed lines) as functions of the reduced exchange length δ/h for different thickness ratio s/h . The inset shows antiferromagnetic domains with sharp walls (b) and *metamagnetic* band defects (c).

$L = 2Xh + 2(X-1)t + s$ is the multilayer thickness) the energy of the metamagnetic phase can be reduced to the following form

$$w = 1 - \frac{4hX}{\pi D} \left[\frac{3}{2} - \ln \left[\frac{\pi h X}{D \cos(\pi q/2)} \right] - \Lambda \right] - 2\eta q, \quad (2)$$

where $\eta = H/(4\pi M) - \delta/(2Xh)$ is the reduced strength of the field, $\tau = (t+h)/h$, $\Lambda = \pi l/(hX) + \gamma(X)$, $\gamma(X) = N^{-2} \sum_{k=1}^{X-1} (N-k) \Upsilon_k(\tau) - \ln(X)$, $\Upsilon_k(\tau) = 2v(\tau k) - v(\tau k+1) - v(\tau k-1)$, and $v(\omega) = \omega^2 \ln(\omega)$. Minimization of energy (2) yields the following solutions [10]

$$D = 4\pi h X / \sqrt{(\eta^*)^2 - \eta^2}, \quad q = (2/\pi) \arcsin(\eta/\eta^*), \quad (3)$$

where $\eta^* = \pi \exp(-\Lambda + 1/2)$. The upper (H_1) and lower (H_2) limiting fields of the metamagnetic region can be written as

$$H_{1,2} = 2\pi M \frac{\delta}{Xh} \pm 4M \exp \left[-\frac{\pi l}{Xh} + \gamma(X) \right]. \quad (4)$$

The metamagnetic transition has been observed in [Co/Pd]/Ru multilayers with $X = 7$ and $N = 2$, $h = 0.4$ nm, $t = 1.8$ nm, and $s = 0.8$ nm [4]. For this multilayer Eqs. (3) yields the domain period $D_0 = 3.43 \mu\text{m}$ in the center of the metamagnetic region H_0 ($q = 0$), and the width of this region $\Delta H = 3$ mT. For the experimental value $H_0 = 0.126$ T and the saturation magnetization $4\pi M = 1.85$ T the equation $H_0 = 2\pi M(\delta/h)$ ($\eta = 0$) yields $\delta = 0.38$ nm. The calculated magnetic phase diagram, using this value of the exchange length, for these [Co/Pd]/Ru systems (Fig. 3, Inset) shows a widening of the metastable region for $X > 7$. In the multilayers with $N \geq 4$ the metamagnetic transition occurs first in the surface layer at $H \propto \delta/h$, and then in the internal layers at higher field $H \propto 2\delta/h$. This kind of two-step transition

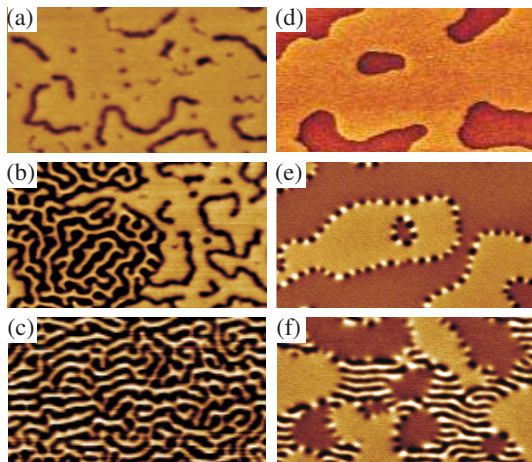


FIG. 4: (Color online) Multidomain patterns observed in Pt(20)[Co(h)Pt(0.7)]₇ Co(h) Ru(0.9)]₁₄ [Co(h)Pt(0.7)]₈ Pt(0.13) multilayers with wedged Co layers after out-of-plane saturation (a-c) and in-plane demagnetization (d-f). ($h = 0.4 - 0.44$ nm for a-c, e,f and $h = 0.36 - 0.4$ nm for d, field of view is $7 \mu\text{m} \times 4 \mu\text{m}$).

in an external field has been observed in [Co/Pt]/Ru systems [7]. Similarly, it also occurs in antiferromagnetically coupled multilayers with in-plane magnetization [12].

The main types of topological defects in the antiferromagnetic ground state include ferro bands (Figs. 3(a), 4 (e)), antiferromagnetic domains with *sharp* domain walls (3 (b), 4 (d)), and metamagnetic bands (3 (c), 4 (a), (b)). For isolated ferro bands the total energy can be written as

$$E = 2M^2h^2 [F(u, \tau) + 2\pi(\delta/h)u] \quad (5)$$

$F(u, \tau) = 2f(a, \tau) - f(u, \tau + 1) - f(u, \tau - 1)$ $f(u, \omega) = (\omega^2 - u^2) \ln(\omega^2 + u^2) - \omega^2 \ln(\omega^2) - 4\omega u \arctan(u/\omega)$. The equation $dE/da = 0$ derives the optimal ferrobands widths (Fig. 3). These solutions are consistent with numerical results in [2, 6]. The equation $d^2E/du^2 = 0$ yields the critical value of the band width $a_{cr} = \sqrt{s^2 + 2sh + h^2/2}$. Substituting this solution into equation $dE/da = 0$ we obtain the equation for the lability line ($o - a - a'$ in Fig. 1). The equation $H = 2\pi M\delta/h_a$ defines the stability limit of the ferrobands in the magnetic phase diagram (line $a - f$ in Fig. 2). Usually the ferrobands split into domains with up and down magnetization creating exotic patterns, named “tiger-tails” [2]. The ferrobands exist within the lability region of the ferrostripe phase (Fig. 1). They collapse into sharp domain walls at the lability $o - a - a'$ and transform into the ferrostripes by unlimited expansion of “tiger-tail” patterns at the transition line $o - b - b'$ as recently observed in [Co/Pt]/Ru multilayers (Fig. 4 (e),(f) and [7]). The phase diagrams of solutions (Figs. 1, 2) explain the evolution of multidomain states observed in [1, 4, 6, 7] and the formation of different remanent states in antiferro-

magnetically coupled multilayers [2, 3, 4, 6, 7]. Usually after out-of-plane saturation magnetic patterns at zero field consist of remnants of the metamagnetic domains ($h < h_c$ in Fig. 3 and Fig. 4, (a)), a mixture of metamagnetic remnants and ferrostripes ($h_c < h < h_b$, Fig. 4 (b)), and regular ferrostripe textures ($h > h_b$, Fig. 4 (c)) (h_a, h_b, h_c are defined on the horizontal axis in Fig. 2). In-plane demagnetization yields a succession of remanent states consisting of antiferromagnetic domains with sharp domain walls ($h < h_a$, Fig. 4, (d)) or a network of ferrobands ($h_a < h < h_b$, Fig. 4, (e)). These domains act as nucleation regions of ferrostripes within the antiferromagnetic state (Fig. 4 (f)). For $h > h_b$ regular ferrostripes create the ground state of the multilayer (Fig. 4, (c)).

In conclusion, we have developed a micromagnetic theory for regular magnetic phases and topological defects arising in perpendicular antiferromagnetically coupled multilayers and explain the formation of different remanent states as consequence of topologically stable defects with different geometry.

The authors thank T. Hauet, J. McCord and R. Schäfer for helpful discussions. Work supported by DFG through SPP1239 (project A08). N.S.K. and A.N.B. thank H. Eschrig for support and hospitality at IFW Dresden.

* Corresponding author ; Electronic address: kiselev@kinetic.ac.donetsk.ua

† Electronic address: u.roessler@ifw-dresden.de

- [1] O. Hellwig, T. L. Kirk, J. B. Kortright, A. Berger, E. E. Fullerton, *Nature Mater.* **2**, 112 (2003).
- [2] O. Hellwig, A. Berger, E. E. Fullerton, *Phys. Rev. Lett.* **91**, 197203 (2003).
- [3] A. Baruth, D. J. Keavney, J. D. Burton, K. Janicka, E. Y. Tsybmal, L. Yuan, S. H. Liou, S. Adenwalla, *Phys. Rev. B* **74**, 054419 (2006).
- [4] Y. Fu, W. Pei, J. Yuan, T. Wang, T. Hasegawa, T. Washiya, H. Saito, S. Ishio, *Appl. Phys. Lett.* **91**, 152505 (2007).
- [5] N. S. Kiselev, I. E. Dragunov, U. K. Röbller, A. N. Bogdanov, *Appl. Phys. Lett.* **91**, 132507 (2007).
- [6] T. Hauet, C. Günther, O. Hovorka, A. Berger, M. Y. Im, P. Fisher, T. Eimüller, O. Hellwig, *Appl. Phys. Lett.*, submitted.
- [7] O. Hellwig, A. Berger, J. B. Kortright, E. E. Fullerton, *J. Magn. Magn. Mater.* **319** 13 (2007).
- [8] A. N. Bogdanov, U. K. Röbller, *cond-mat/0606671* (2006).
- [9] A. Hubert, R. Schäfer, *Magnetic Domains* (Springer-Verlag, Berlin, 1998).
- [10] A. N. Bogdanov, D. A. Yablonskii. *Fiz. Tverd. Tela* **22**, 680 (1980) [*Sov. Phys. Solid State* **22**, 399 (1980)].
- [11] E. Strykowski, N. Giordano, *Adv. Phys.* **26**, 487 (1977).
- [12] U. K. Röbller, A. N. Bogdanov, *Phys. Rev. B* **69**, 094405 (2004).